

# A Photoelectric Method for Analyzing NO-Induced Apoptosis in Cultured Neuronal Cells

Chunyang Zhang,<sup>+</sup> Taotao Wei,<sup>++</sup> Hui Ma,<sup>\*+</sup> Chang Chen,<sup>++</sup> Wenjuan Xin,<sup>++</sup> and Dieyan Chen<sup>+</sup>

<sup>+</sup> Molecular and Nano Sciences Laboratory, Department of Physics, Tsinghua University, Beijing 100084, P.R. China  
e-mail: mahui@tsinghua.edu.cn

<sup>++</sup> Department of Molecular and Cellular Biophysics, Institute of Biophysics, Chinese Academy of Sciences, Beijing 100101, P.R. China

Received: January 6, 2000

Final version: March 2, 2000

## Abstract

A photoelectric method for analyzing NO-induced apoptosis in cultured neuronal cells is presented. By integrating ITO (a transparent electrode of indium-tin oxide coated with borosilicate) with a layer of primary rat cerebellar granule cells and a photoelectric-current-measuring system, a cytosensor for measuring photoelectric current of neuronal cells was formed. The cells generated an anode photoelectric current under white light (200–800 nm). The amplitude of the photoelectric current was related to the cell number, the light intensity and the cell viability. During neuronal apoptosis, the decrease of the photoelectric current was in accordance with the decrease of the cell viability, the loss of mitochondrial transmembrane potential, and the fragmentation of DNA. This photoelectric method may provide a simple and sensitive way to study electron-transfer mechanism during NO-induced neuronal apoptosis.

**Keywords:** Photoelectric current, Apoptosis, Neuronal cells, Nitric oxide, Mitochondrial transmembrane potential

## 1. Introduction

Apoptosis is distinguished from necrosis by characteristically morphological and biochemical changes, including compaction and fragmentation of the chromatin, activation of certain protease and nuclease, cytoskeleton breakdown, and loss of mitochondrial transmembrane potential [1–3]. Physiological apoptosis plays an important role in the development of the central nervous system. Inappropriate apoptosis leads to some neurodegenerative diseases including amyotrophic lateral sclerosis, Alzheimer's disease, Parkinson's disease and various forms of cerebellar degeneration [4, 5]. More and more evidences have suggested that nitric oxide (NO) plays an important role in apoptosis [6, 7]. NO is a highly reactive free radical that facilitates a number of functions including neurotransmission, synaptic plasticity and memory in the mammalian central nervous system [8, 9]. When produced with superoxide concurrently, NO converts to peroxynitrite at very high rates ( $k \geq 6.7 \times 10^9 \text{ M}^{-1} \text{ s}^{-1}$ ), which is a potent oxidant and acts as a pathological mediator in some neurodegenerative disorders [10].

The detection methods of neuronal apoptosis include enzyme and protein analysis [11, 12], morphological observation [5, 13], DNA electrophoresis [14], TUNEL staining (Terminal deoxynucleotidyl transferase (TdT)-mediated dUTP-biotin nick end labeling) [15] and flow cytometry [16]. But, so far, few sensitive and simple methods are capable of studying electron-transfer mechanism during neuronal apoptosis.

Many important processes in living cells have electrochemical characteristics. A living cell can be properly described as an electrochemical dynamic system. Electron generation and electron transfer on the interface do exist in living cells [17]. Many electrochemical methods have been used in studying intact living cells, such as tracking the morphological change of adherent cells using an electric impedance sensing system [18, 19], studying the response of cells to various chemical substances by monitoring the acidification of living cells to their environment [20, 21]. Such applications of electrochemical methods have greatly enriched our knowledge on the electrochemistry of living cells.

The photoelectric method for studying living cells may throw new light on the electrochemistry of living cells. We had developed a photoelectric method to detect the photoelectric current of living cells responding to light with ITO technology [22]. In this article, we used this photoelectric method to study NO-induced apoptosis in primary cultures of rat cerebellar granule cells.

## 2. Experimental

### 2.1. Materials

Albino Wistar rats were purchased from Beijing Medical University, China. Cell culture plastic ware was purchased from Corning Costar (Acton, MA, USA). ITO conductor glasses were gifts from Prof. Huang C. H., Peking University, China. Dulbecco's modified Eagle medium (DMEM), cell culture supplements, fetal bovine serum and trypsin (1:250) were products of Gibco BRL (Grand Island, NY, USA). *S*-nitroso-*N*-acetyl-penicillamine (SNAP), 3-[4,5-dimethylthiazol-2-yl]-2,5-diphenylterazolium bromide (MTT), acridine orange, rhodamine 123 and poly-L-lysine were purchased from Sigma (St. Louis, MO, USA). Other reagents were of analytical grade.

### 2.2. Cell Culture and Treatment with NO

Primary cultures of rat cerebellar granule cells were prepared following the previously described procedure [23]. Briefly, cerebella from 7-day-old Albino Wistar rats were dissected out, rinsed with Hanks' balanced salt solution, and dissociated by mild trypsinization. The rat cerebellar granule cells were plated on 35 mm Petri dishes ( $2 \times 10^6$  cells/mL, 2 mL/dish) or 24-well multidishes ( $2.5 \times 10^6$  cells/mL, 2 mL/well) which were coated with poly-L-lysine. In photoelectric experiments, the cells were plated on ITO conductor glass coated with poly-L-lysine in 35 mm Petri dishes. Cell density was estimated by trypan blue exclusion on a hemacytometer slide under a phase contrast

microscope. Culture medium consisted of DMEM supplemented with 19.6 mM KCl, 2 mM glutamine, 10 mM *N*-2-hydroxyethylpiperazine-*N'*-2-ethanesulfonic acid and 10% (v/v) fetal bovine serum. The cells were maintained at 37 °C in a humidified 5% CO<sub>2</sub>-95% air atmosphere. After the cells were cultured for 48 h, aliquots of SNAP solution (NO donor) were rapidly added to the wells, then the cells were incubated for 24 h.

### 2.3. Photoelectric Current Measurement

The photoelectric measurement system consisted of three electrodes. The working electrode was made of ITO conductor glass with the illuminated area of 0.5 cm<sup>2</sup>, the counter electrode was a platinum electrode and the reference electrode was a saturated calomel electrode. The voltage of working electrode with respect to the reference electrode was 0 V vs. standard calomel electrode (SCE) in all the experiments. Phosphate-buffered saline (PBS) was used as electrolyte in the measuring system and as washing solution of the cells. The photoelectric current measurements were performed with a Model 600 voltage analyzer (CH instruments Inc., TN, USA). The light source was a 500-W xenon lamp. To reduce the heating effects due to light absorption, we inserted an infrared filter in the light path to remove the infrared light.

After treatment with SNAP for 24 h, the ITO conductor glass with a layer of cells was removed from culture medium and washed with PBS, then the ITO conductor glass was mounted in the light path. The dark current ( $I_{\text{light off}}$ ) was first measured with light off, then the light current ( $I_{\text{light on}}$ ) was measured with light on. The photoelectric current ( $\Delta I$ ) was the difference between  $I_{\text{light on}}$  and  $I_{\text{light off}}$  ( $\Delta I = I_{\text{light on}} - I_{\text{light off}}$ ).

### 2.4. MTT Assay

The viability of cells was assessed by MTT assay [24]. MTT can be reduced to formazan by mitochondrial respiratory enzymes, and the amount of formazan was related to the cell viability. After the cells were treated with SNAP for 24 h, 40  $\mu$ L of MTT solution (50 mg/mL in PBS) were added to each well on the 24-well multidishes, and incubated at 37 °C for 30 min. Then 600  $\mu$ L of solubilization solution (50% dimethylformamide, 20% sodium dodecyl sulfate, 1% acetyl acid and pH 3.5) was added to the well and mixed for 10 min. The absorption at 570 nm was measured.

### 2.5. Detection of DNA Fragmentation

After exposure of cells to SNAP for 24 h, cytosolic DNA fragments were quantified using a cell death detection ELISA<sup>PLUS</sup> kit (Boehringer Mannheim, Cat. No. 1774425) as previously described [25]. An enrichment factor, which represented the enrichment of nucleosomes in the cytoplasm of cells, was used as an index of DNA fragmentation.

### 2.6. Nuclear Morphological Observation

Following SNAP treatment, cells were stained with 1  $\mu$ M acridine orange and imaged with a Bio-Rad MRC 1024MP laser

scanning confocal microscope at 488 nm excitation and 520 nm emission.

### 2.7. Measurement of Mitochondrial Transmembrane Potential

The mitochondrial transmembrane potential was measured with flow cytometry using rhodamine 123 as a mitochondrial energization-sensitive fluorescence probe [26]. The intensity of rhodamine 123 fluorescence is directly related to the mitochondrial transmembrane potential [27]. Following treatment with SNAP for 3 h, cells were treated with 0.02% trypsin-20  $\mu$ g/mL DNase I, washed twice with Locke's solution, and stained with 1  $\mu$ M rhodamine 123 in Locke's solution at 37 °C for 30 min. After being washed twice with Locke's solution, cells were analyzed with a Becton-Dickinson FACS 420 flow cytometer at 488 nm excitation and 520 nm emission.

The mitochondrial rhodamine 123 fluorescence was also observed directly with a laser scanning confocal microscope [28]. After treatment with SNAP for 3 h, cells were stained with 1  $\mu$ M rhodamine 123 and imaged with a Bio-Rad MRC 1024MP laser scanning confocal microscope at 488 nm excitation and 530 nm emission.

## 3. Results and Discussion

### 3.1. The Relationship of Photoelectric Current of Rat Cerebellar Granule Cells with Light Intensity and Cell Number

Figure 1 showed a typical photoelectric current of rat cerebellar granule cells responding to white light (200–800 nm). In six parallel experiments, the photoelectric current of ITO without cells (the background) was in the range of  $-48.0$  nA to  $-56.7$  nA. However, the photoelectric current of ITO with cells was in the range of  $-92.5$  nA to  $-102.5$  nA. If the background was subtracted, the net photoelectric current of rat cerebellar granule cells was in the range of  $-39.0$  nA to  $-54.5$  nA (Table 1). These results indicated that the photoelectric method was capable of detecting the photoelectric current of rat cerebellar granule cells.

To observe the effect of light on the photoelectric current of living cells, we studied the influence of light intensity upon the photoelectric current (Fig. 2). When the light was very weak

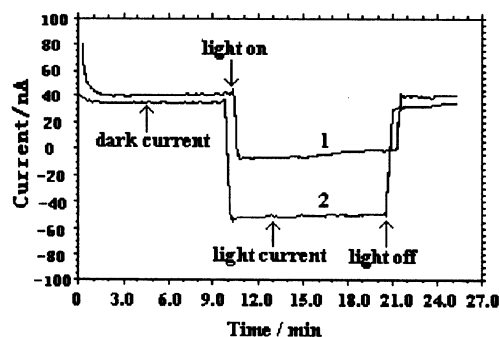


Fig. 1. Photoelectric current of rat cerebellar granule cells responding to white light. 1) Photoelectric current of ITO without cells; 2) Photoelectric current of ITO with cells.

Table 1. Photoelectric current of rat cerebellar granule cells responding to white light. The light intensity was  $121.4 \text{ mW cm}^{-2}$ .  $\Delta I_f$ : photoelectric current of ITO without cells.  $\Delta I_C$ : photoelectric current of ITO with cells.  $\Delta I_C - \Delta I_f$ : net photoelectric current of the cells.

ITO number	1	2	3	4	5	6
$\Delta I_f$ (nA)	-55.0	-53.5	-51.5	-49.6	-56.7	-48.0
$\Delta I_C$ (nA)	-96.8	-92.5	-97.6	-94.7	-100.6	-102.5
$\Delta I_C - \Delta I_f$ (nA)	-41.8	-39.0	-46.1	-45.1	-43.9	-54.5

( $2.0 \text{ mW cm}^{-2}$ ), no measurable photoelectric current was obtained. With increasing light intensity, the photoelectric current increased. However, Figure 2 showed that the photoelectric current saturated at high light intensity, and increasing light did not increase the photoelectric current significantly.

We also studied the relationship between the photoelectric current and the cell number. With increasing cell number, the photoelectric current increased (Fig. 3). This result indicated that the photoelectric current had a positive relationship with the cell number. It should be noted that zero cell number did not correspond to zero photoelectric current in Figure 3. This was due to the background photoelectric current of ITO (see Fig. 1)

### 3.2. Photoelectric Analysis of NO-Induced Apoptosis of Rat Cerebellar Granule Cells

Figure 4 showed the variance of photoelectric current and cell viability with SNAP concentration (SNAP is a commonly used NO donor. It can induce apoptosis by releasing NO [29, 30]). With increasing SNAP concentration, both the cell viability and photoelectric current decreased (Fig. 4). This result indicated that the change of photoelectric current of the cells was related to the cell viability.

To assess whether cerebellar granule cells underwent apoptosis after exposure to NO donor SNAP, we examined the nuclear morphology with laser scanning confocal microscopy and DNA nucleosomal fragmentation with ELISA. Morphological observation showed typical apoptotic characteristics such as chromatin condensation and formation of apoptotic body in SNAP-treated neuronal cells (Fig. 5b, c). Quantitative detection of DNA fragmentation indicated that exposure to NO donor caused a marked increase in histone-associated DNA fragments (mono- and

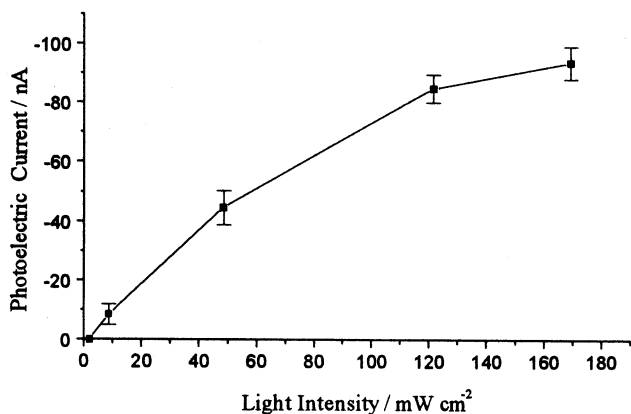


Fig. 2. Influence of light intensity upon the photoelectric current of the cells. Data are mean  $\pm$  SD of 3 different experiments.

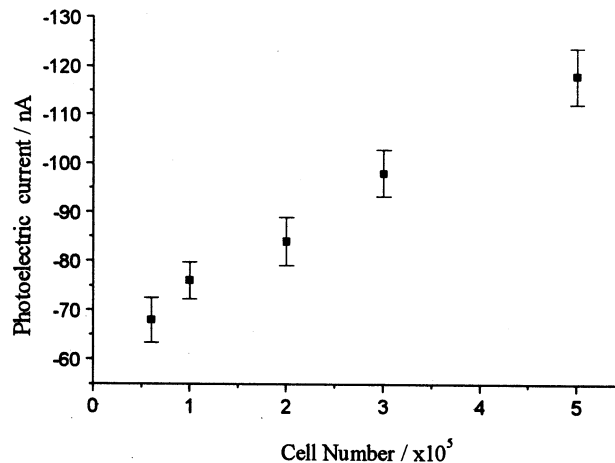


Fig. 3. Variance of photoelectric current with cell number. The light intensity was  $121.4 \text{ mW cm}^{-2}$ . Data are mean  $\pm$  SD of 3 different experiments.

oligonucleosomes) (Fig. 6), the formation of mono- and oligonucleosomes was a well-accepted biochemical characteristic of apoptosis [25]. Both histological evidence (nuclear morphology, Fig. 5b, c) and biochemical evidence (DNA nucleosomal fragmentation, Fig. 6) indicated that exposure to NO donor SNAP induced apoptosis in rat cerebellar granule cells. Comparing Figure 4 with Figure 6, we found that the decrease of photoelectric current was in accordance with the increase of DNA fragments during neuronal apoptosis induced by NO.

A living cell can be properly described as an electrochemical dynamic system with electron generation and electron transfer on the interface [17]. Szent-Gyorgyi suggested the possibility of semiconduction of electrons within proteins more than 50 years ago [31]. Very recently, the likelihood of electron transfer through the DNA double helix had been demonstrated [32, 33]. It was also demonstrated that microtubules possessed piezoelectric properties, which may play a quite important role in electrons transfer [34]. Moreover, cytoskeleton, which existed within the cytoplasm and extended within nucleus and the plasma membrane, formed a complex network of electron transfer within living cells [17]. Therefore, we assumed that the nuclear DNA,

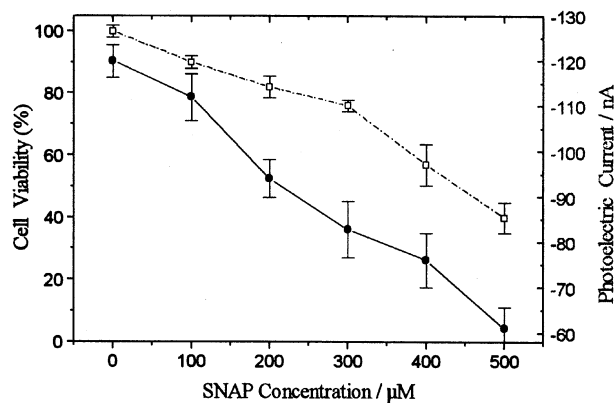


Fig. 4. Variance of the photoelectric current (●) and the cell viability (□) with SNAP concentration. After the cerebellar granule cells were incubated with SNAP for 24 h, the cell viability was determined by MTT assay, and the photoelectric current was measured with a light intensity of  $121.4 \text{ mW cm}^{-2}$ . Data are mean  $\pm$  SD of 6 different experiments.

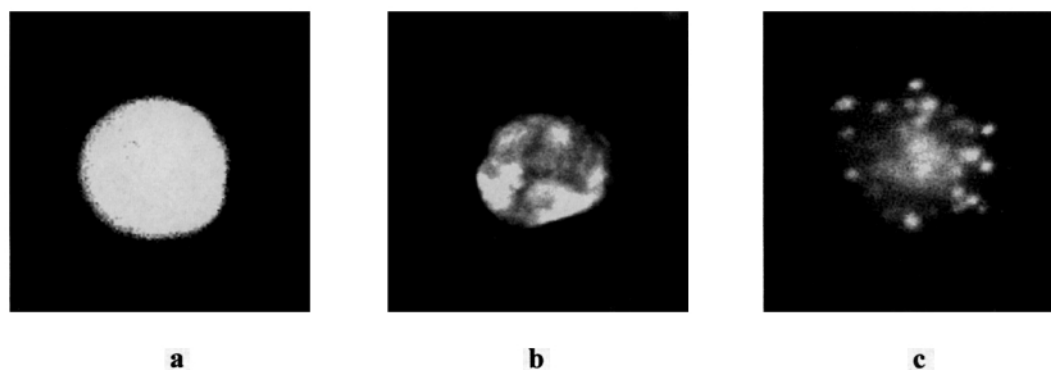


Fig. 5. Variance of nuclear morphology observed with laser scanning confocal microscopy. a) Normal cerebellar granule cell with intact nuclear; b) cell with chromatin condensation after treatment with 500  $\mu\text{M}$  SNAP for 12 h; c) cell with fragmented nuclear after treatment with 500  $\mu\text{M}$  SNAP for 24 h.

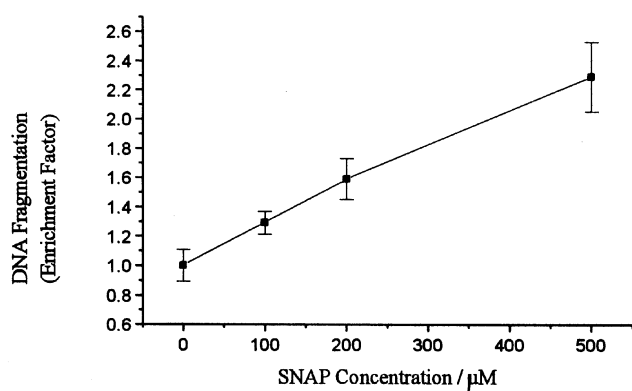


Fig. 6. Quantitative determination of DNA fragmentation with ELISA. After the cerebellar granule cells were incubated with NO donor SNAP for 24 h, the histone-associated DNA fragments (mono- and oligonucleosomes) were quantified with ELISA. An enrichment of nucleosomes in the cytoplasm of cells was employed as an index of DNA fragmentation. Data are mean  $\pm$  SD of 3 different experiments.

microtubules and cytoskeleton may serve as ‘electric wires’ for photo-induced electron transfer within living cells. Apoptosis resulted in nuclear DNA fragmentation and morphological changes including cytoskeleton breakdown [1–3], which led to the alteration of electron transfer within the cells, and the alteration of electron transfer can be described by the change of photoelectric current. So this photoelectric method may provide a

simple way to study the electron-transfer mechanism during neuronal apoptosis induced by NO.

Depolarization of mitochondrial membrane was an early event of apoptosis [35]. To detect whether the decrease of photoelectric current was consistent with the loss of mitochondrial transmembrane potential, we measured the mitochondrial transmembrane potential by staining with rhodamine 123. The rhodamine 123 uptake visualized with laser scanning confocal microscopy showed that the mitochondrial transmembrane potential decreased with increasing SNAP concentration (Fig. 7a–c). The loss of mitochondrial transmembrane potential was also quantitatively measured by determining the rhodamine 123 fluorescence intensity with flow cytometry. Results from flow cytometry showed the dose dependent decrease of rhodamine 123 fluorescence with SNAP concentration (Fig. 8). The loss of mitochondrial transmembrane potential resulted from the dysfunction of mitochondria induced by NO. NO diffused across the plasma membrane and the mitochondrial membrane, reacted with thiol group, iron-sulfur clusters and heme proteins, and thus influenced the activity of enzymes [36, 37]. Moreover, NO can react with superoxide to form peroxynitrite at very high rates. Peroxynitrite may oxidize the cysteine and tyrosine residues of enzymes and inactivate the mitochondrial enzymes irreversibly [38]. The dysfunction of mitochondria led to the changes of electron transfer in the mitochondrial electron transport chain, which might influence the photoelectric current of cells. Comparing Figure 4 with Figure 8, we found that both the photoelectric current and rhodamine 123 fluorescence intensity

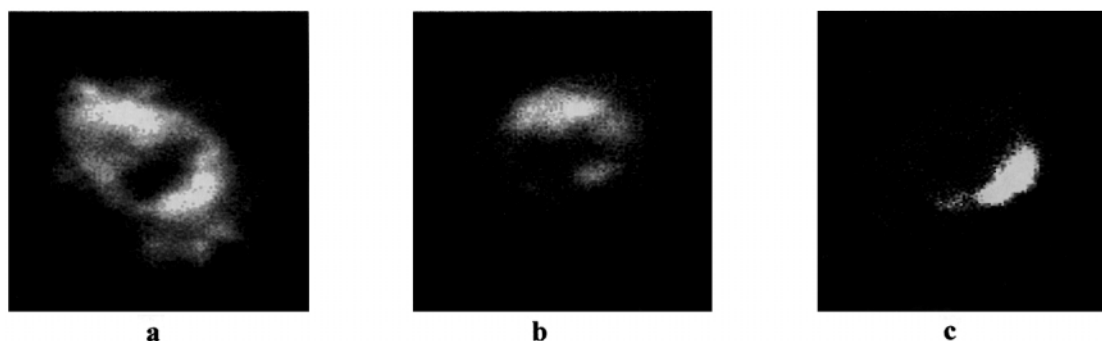


Fig. 7. Variance of mitochondrial transmembrane potential observed with laser scanning confocal microscopy. a) Normal cerebellar granule cell; b) cell exposed to 200  $\mu\text{M}$  SNAP for 3 h; c) cell exposed to 500  $\mu\text{M}$  SNAP for 3 h.

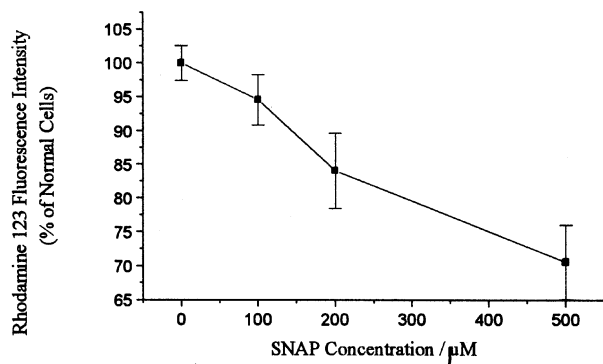


Fig. 8. NO-induced mitochondrial transmembrane potential decrease in cerebellar granule cells. After the cerebellar granule cells were incubated with NO donor SNAP for 3 h, the mitochondrial transmembrane potential was measured with flow cytometry using rhodamine 123 as a fluorescence probe. Data are mean  $\pm$  SD of 3 different experiments.

decreased with increasing SNAP concentration. This result indicated that the decrease of photoelectric current was in accordance with the loss of mitochondrial transmembrane potential during neuronal apoptosis induced by NO.

#### 4. Conclusions

A novel cytosensor for measuring photoelectric current of neuronal cells was devised and used for analyzing NO-induced neuronal apoptosis. During neuronal apoptosis, the decrease of photoelectric current was in accordance with the decrease of cell viability, DNA fragmentation and the loss of mitochondrial membrane potential. This photoelectric method may provide a simple and sensitive way to study the electron-transfer mechanism during NO-induced neuronal apoptosis.

#### 5. Acknowledgements

This project was supported by the 985 Fund of Tsinghua University and the grant from The National Natural Science Foundation of China (No. 39800035).

#### 6. References

- [1] J.F.R. Keer, A.H. Willie, A.R. Currie, *Br. J. Cancer* **1972**, *26*, 239.
- [2] J.F.R. Keer, C.M. Winterford, B.V. Harmon, *Cancer* **1994**, *73*, 2013.
- [3] D.R. Green, J.C. Reed, *Science* **1998**, *281*, 1309.
- [4] C.B. Thompson, *Science* **1995**, *267*, 1456.
- [5] C. Charriaut-Marlangue, D. Aggoun-Zouaoui, *Trends Neurosci.* **1996**, *19*, 109.
- [6] M.P. Murphy, *Biochim. Biophys. Acta* **1999**, *1411*, 401.
- [7] L. Bosca, S. Hortelano, *Cell Signal.* **1999**, *11*, 239.
- [8] C. Hölscher, *Trends Neurosci.* **1997**, *20*, 298.
- [9] R.D. Hawkins, *Neuron* **1996**, *16*, 465.
- [10] S.S. Gross, M.S. Wolin, *Annu. Rev. Physiol.* **1995**, *57*, 737.
- [11] L.I. Benowitz, N.I. Perrone-Bizzozero, R.L. Neve, *Prog. Brain Res.* **1990**, *86*, 309.
- [12] G. Keilhoff, G. Wolf, *Neuroreport* **1993**, *5*, 129.
- [13] J.A. Watt, C.J. Pike, A.J. Walencewicz-Wasserman, C.W. Cotman, *Brain Res.* **1994**, *661*, 147.
- [14] J. Gong, F. Traganos, Z. Darzynkiawioz, *Anal Biochem.* **1994**, *218*, 314.
- [15] Y. Gavieli, Y. Sherman, S.A. Ben-Sasson, *J. Cell Biol.* **1992**, *119*, 493.
- [16] L.I. Huschtscha, T.M. Jeitner, C.E. Andersson, W.A. Bartier, M.H.N. Tattersall, *Exp. Cell Res.* **1994**, *212*, 161.
- [17] M.N. Berry, M.B. Grivell, *An Electrochemical Description of Metabolism, in Bioelectrochemistry of Cells and Tissues* (Eds: D. Walz, H. Berry, G. Milazzo), Birkhäuser, Basel **1995**, 134–158.
- [18] I. Giaever, G.R. Keese, *Proc. Natn. Acad. Sci. U.S.A.* **1991**, *88*, 7896.
- [19] I. Giaever, G.R. Keese, *Nature* **1993**, *66*, 591.
- [20] H.M. McConnell, J.C. Owicki, J.W. Parce, D.C. Miller, G.T. Baxter, H.G. Wada, S. Pitchford, *Science* **1992**, *257*, 1906.
- [21] J.C. Owicki, J.W. Parce, *Biosens. Bioelectron.* **1992**, *7*, 255.
- [22] Y.X. Ci, C.Y. Zhang, J. Feng, *Bioelectrochem. Bioenerg.* **1998**, *45*, 247.
- [23] Y.C. Ni, B.L. Zhao, J.W. Hou, W.J. Xin, *Neurosci. Lett.* **1996**, *214*, 115.
- [24] M.B. Hansen, S.E. Nielsen, K. Berg, *J. Immunol. Methods* **1989**, *119*, 203.
- [25] M. Sandoval, X.J. Zhang, X.P. Liu, E.E. Mannick, D.A. Clark, M.J.S. Miller, *Free Radic. Biol. Med.* **1997**, *22*, 489.
- [26] R.K. Emaus, R. Grunwald, J.J. Lemaster, *Biochim. Biophys. Acta* **1986**, *850*, 436.
- [27] R.J. Mark, J.N. Keller, I. Kruman, M.P. Mattson, *Brain Res.* **1997**, *756*, 205.
- [28] J. Yang, X. Liu, K. Bhalla, C.N. Kim, A.M. Ibrado, J. Cai, T. Peng, D.P. Jones, X. Wang, *Science* **1997**, *275*, 1129.
- [29] S. Kojima, *Anticancer Res.* **1997**, *17*, 929.
- [30] E. Nishio, K. Fukushima, M. Shiozaki, Y. Watanade, *Biochem. Biophys. Res. Commun.* **1996**, *221*, 163.
- [31] Szent-Gyorgi, *Science* **1941**, *93*, 609.
- [32] G.J. Murphy, M.A. Arkin, Y. Jenkins, N.D. Ghatlia, S.H. Bossmann, N.J. Turro, J.K. Barton, *Science* **1993**, *262*, 1025.
- [33] M.D. Puraggan, C.V. Kamar, N.J. Tarro, J.K. Barton, *Science* **1988**, *24*, 1645.
- [34] R.L. Margolis, L. Wilson, *Nature* **1981**, *293*, 703.
- [35] N. Zamzami, S.A. Susin, P. Marchetti, T. Hirsch, I. GomezMonterry, M. Castedo, G. Kroemer, *J. Exp. Med.* **1996**, *183*, 1533.
- [36] J.P. Bolaños, S. Penchen, S.J.R. Heales, J.M. Land, J.B. Clark, *J. Neurochem.* **1994**, *63*, 910.
- [37] J.P. Bolaños, S.J.R. Heales, S. Penchen, J.E. Barker, J.M. Land, J.B. Clark, *Free. Radic. Biol. Med.* **1996**, *21*, 995.
- [38] J.P. Bolaños, S.J.R. Heales, J.M. Land, J.B. Clark, *J. Neurochem.* **1995**, *64*, 1965.